Wave Breaking Turbulence at the Offshore Front of the Columbia River Plume

Jim Thomson[1], Alex R. Horner-Devine[1], Seth Zippel[1],Curtis Rusch[1], W. Geyer[2]

Corresponding author: J. Thomson, Applied Physics Laboratory, University of Washington, 1013 NE 40 St, Seattle WA, 98105, USA. (jthomson@apl.uw.edu)

[1]University of Washington, Seattle, Washington, USA.

[2]Woods Hole Oceanographic Institution, Woods Hole, Mass., USA.

Observations at the Columbia River plume show that wave breaking is an important source of turbulence at the offshore front, which may contribute to plume mixing. The lateral gradient of current associated with the plume front is sufficient to block (and break) shorter waves. The intense whitecapping that then occurs at the front is a significant source of turbulence, which diffuses downward from the surface according to a scaling determined by the wave height and the gradient of wave energy flux. This process is distinct from the shear-driven mixing that occurs at the interface of river water and ocean water. Observations with and without short waves are examined, especially two cases in which the background conditions (i.e., tidal flows and river discharge) are otherwise identical.

1. Introduction

The local effects of waves and wave breaking on river plumes and the mixing of estaurine waters is largely unknown. *Gerbi et al.* [2013] present a numerical study of whitecap effects on the Hudson River plume and find that the turbulence supplied by short-wave breaking is sufficient to increase the plume depth h_p and slow the offshore expansion of the plume. *Gerbi et al.* [2013] show that interfacial gradients in salinity and velocity (i.e., vertical shear) are reduced by the addition of turbulence at the surface. This requires that the surface turbulence from the breaking waves diffuses downwards (e.g., *Craig and Banner* [1994]) and reaches the base of the plume. This description is largely a vertical balance, which then controls the lateral evolution of the plume.

A river plume will, in turn, affect the waves. This is primarily a lateral process, in which waves incident from offshore (weak or no current) are shortened by an opposing current at the edge of plume such that the absolute frequency ω is conserved

$$\omega = \sigma + \vec{u} \cdot \vec{k}, \tag{1}$$

where $\vec{u}$ is the plume current, $\vec{k}$ is the wavenumber, and σ is the intrinsic frequency given by the linear finite-depth dispersion relation, $\sigma^2 = gk\tanh(kd)$. Wave blocking occurs when an opposing current $\vec{u}$ equals half of the group velocity, $u = -\frac{1}{2}c_g = -\frac{1}{2}\frac{\partial\omega}{\partial\vec{k}}$ [*Mei*, 1989], however previous studies have shown that waves typically over-steepen and break before the actual blocking condition is reached [*Chawla and Kirby*, 2002]. For monochromatic waves, steepness of the waves can be approximated by Ak, where A is the wave amplitude (equal to half the height H) and k is the scalar magnitude of the wavenumber vector and must become larger (i.e., a shorter wave) in the presence of an opposing current u. The convention for a random wave field is to use significant wave height, H_s, and wavenumber at the peak of the wave spectrum, k_p, and in this convention deep-water wave breaking (i.e., whitecapping) is commonly observed for $\frac{1}{2}H_s k_p \sim 0.1$ [*Banner et al.*, 2000].

Here, we present observations of wave breaking effects at the offshore front of the Columbia River plume. The Columbia River plume has been studied by many previous authors, in particular *Kilcher and Nash* [2010] who describe the shear-driven interfacial mixing as the plume spreads offshore and *McCabe et al.* [2008] who describe the salt fluxes of the spreading plume in a Lagranian frame. The transformation of waves at the Columbia River mouth has also been studied by previous authors, in particular *Gonzalez and Rosenfeld* [1984] who describe the refraction and focusing of waves in the presence of the opposing currents and *Kassem and Ozkan-Haller* [2012] who show increased wave heights and steepness in the presence of the opposing currents. In contrast to the previous works, our study is limited to an assessment of the wave-driven processes at the edge of the river plume as it spreads offshore during ebb tides, in particular where the vertical and lateral processes collide. We consider two cases with similar tidal and river conditions, but with differing wave conditions.

2. Data Collection

Data were collected using freely drifting SWIFTs (Surface Wave Instrument Floats with Tracking), which were deployed inside the mouth of the Columbia River (i.e., between the jetties) and allowed to drift offshore during ebb tides. The SWIFTs are designed for wave-following measurements of near-surface turbulence and are described in *Thomson* [2012]. The original version uses an up-looking pulse-coherent Doppler sonar for turbulence measurements, in particular profiles of the turbulent dissipation rate, $\epsilon(z)$, estimated using the structure function of velocity fluctuations within 0.6 m of the water surface ($z = 0$ m). Here, a down-looking version of the SWIFT was also used, which measures currents and shear from 1.9 to 20 m below the water surface. SWIFTs also measure wave spectra, following the GPS-based method of *Herbers et al.* [2012], and winds, using an ultrasonic anemometer (Airmar PB 200) mounted at 0.9 m above the surface. Conductivity sensors (Onset HOBO) were added to the SWIFTs for this experiment at 0.5 m below the surface. Finally, an onboard camera collecting images at 1 Hz is used to count breaking waves observed by each SWIFT [*Rusch et al.*, 2014]. All SWIFT observations are averaged and merged to five-minute ensemble values.

The data for this study were collected on morning ebbs of the 24th and 25th May 2013. The SWIFTs were deployed in pairs of up-looking and down-looking versions and allowed to drift offshore until becoming caught in the plume front and recovered several hours later. On both days, the drifts began from navigation buoy #12 just after peak ebb (predicted as 04:42 and 05:28 PDT, respectively). The SWIFT pairs stayed within 100 m of each other during transits of up to 50 km offshore. The SWIFTs became entrained in the sharp front that commonly forms at the edge of the spreading plume around 20 km offshore, and then turned north with the plume. The tracks from May 24th and 25th are shown in Figure 1.

On both days the surface currents at the river mouth were approximately 2 m/s and surface currents offshore (in the front) were approximately 1 m/s, as measured by the drift velocity of the SWIFTs. On both days the river stage was similar, with the nearest upstream USGS gage (#14246900) reporting approximately 3 m and the USGS gage immediately downstream of the Bonneville dam (#14128870) reporting 6.7 to 7.1 m over the two day period. The discharge at Bonneville dam ranged from 321,600 to 285,700 cfs during these two days. The tidal elevation drops at Tongue Point (Astoria, OR) were 3.3 and 3.4 m, respectively.

Wave and wind conditions, as measured by the SWIFTs, were notably different between the two days. On May 24th there was a moderate swell and the seas were calm. On May 25th the swell was somewhat reduced, but there was a strong wind sea from the south, arising from approximately 10 m/s southerly winds.

Additional wave data was collected by a Datawell Waverider buoy maintained by the Coastal Data Information Program (CDIP station 179), moored offshore at the Astoria Canyon (46.1328, -124.6455). This position is outside of the plume for the data considered here, and thus a measure of the incident wave field before it encounters the currents associated with the plume.

3. Analysis

3.1. Wave Breaking at the Plume Front

As shown in Figure 1 with a picture taken from the R/V Oceanus during the same research cruise, wave breaking can be vigorous at the offshore edge of the river plume. This is confirmed by the breaking waves counted using the images onboard each SWIFT, which range from 5 to 10 breakers per five-minute ensemble on May 25th. This is in contrast to the calm conditions at the offshore edge of the river plume on May 24th, when there were only 0 to 1 breakers per five-minute ensemble. These breaker counts are converted to a breaking fraction

$$Q_b = \frac{N}{\bar{\sigma}\mathcal{T}}, \tag{2}$$

where N is the number of breakers in a given amount of time $\mathcal{T} = 300$ s that pass at an energy-weighted average intrinsic frequency $\bar{\sigma}$.

The breaking fractions (or rates) observed on May 25th far exceed the whitecap rates expected for the observed 10 m/s winds [*Thomson et al.*, 2009], and this enhanced breaking is a result of the strong wave-current interaction at the plume edge. For a 1 m/s plume current, wave blocking in deep-water occurs for frequencies of $f = 2\pi\omega > 0.38$ Hz and breaking via oversteepening can be expected for frequencies of $f = 2\pi\omega > 0.2$ Hz (assuming $H_s = 1$ m and $\frac{1}{2}H_s k_p$ is limited to < 0.1 for the wind-chop portion of the wave spectrum). The effect is clear in the observed wave energy density spectra in Figure 1, where the affected frequencies are annotated. On May 24th, the wave energy density at these frequencies is similar within the plume (SWIFT measured) and offshore of the plume (CDIP measured), because it is a calm day and there is very little energy at those frequencies. On May 25th, the wave energy density at these frequencies is reduced within the plume (SWIFT measured) relative to offshore of the plume (CDIP measured), because these waves break when they encounter the currents at the plume edge. This assumes deep water and neglects adjustments to the wave-current interactions for the vertical shear of the plume currents (e.g., *Dong and Kirby* [2012]), both of which are justified for short waves.

Thus, the difference between the two days (one windy, the other calm) is not that there are whitecaps over the whole plume, but rather that there are short waves incident on the plume which are blocked (or broken, actually) by the horizontally sheared surface current. This creates a narrow region of intense wave dissipation at the expanding front.

The gradient of wave energy flux $\frac{dF}{dx}$ is the quantification of the wave energy loss rate in a breaking region of lateral width dx, and is calculated by a wave energy spectrum in deep water via

$$\frac{dF}{dx} = \frac{dEc_g}{dx} = \frac{d}{dx}\int E(f)\frac{g}{2f}df. \tag{3}$$

On May 24th, there is a negligible $\frac{dF}{dx}$ across the plume front for the frequency range $0.2 < f < 0.7$ Hz. On May 25th, by contrast, there is a notable $\frac{dF}{dx}$ across the plume front (i.e., the difference between the blue and black lines in Figure 1b). Assuming a frontal region of $dx = 100$ m [*Nash and Moum*, 2005], the wave dissipation rate in the front on May 25th is similar to a surf zone at a small shore break. The wave energy flux gradient will be used in a model of the surface turbulence, and a constant value will be used for each day because the offshore CDIP wave spectra are only available on an hourly basis (as opposed to the five-minute spectra from the SWIFTs).

3.2. Surface Turbulence Measurements

SWIFT measurements of waves, surface turbulence, and plume currents for both days are shown versus along track distance in Figure 2. The up-looking turbulence profiles $u'(z)$ collected by the SWIFTs are processed to obtain the vertical structure function $D(z, r)$, where z is the vertical location ($z = 0$ is the instantaneous free surface) and r is the distance between velocity fluctuations as [*Wiles et al.*, 2006]

$$D(z, r) = \overline{(u'(z) - u'(z + r))^2}. \tag{4}$$

The structure function approach is distinct from the more conventional frequency spectral method, because it does not require the assumption of an advected frozen field (i.e., Taylor's hypothesis). Assuming a cascade of isotropic eddies in the inertial subrange, $D(z, r)$ has the form $\mathcal{A}r^{2/3}$ at each z level in the profile, the corresponding energy dissipation rate is given by [*Wiles et al.*, 2006]

$$\epsilon(z) = \left(\frac{\mathcal{C}_v^2}{\mathcal{A}(z)} \right)^{3/2}, \tag{5}$$

where $\mathcal{C}_v^2$ is a constant and $\mathcal{A}(z)$ is determined for each z from by $r^{2/3}$.

On both days the SWIFTs cross the bar at approximately $x = -8$ km and reach the plume front at approximately $x = -25$ km (Figure 1). Although the wave height transformation via shoaling and focusing at the bar is dramatic on both days, these are predominately long waves (swell) and are not steep enough to break. This is confirmed by the breaker counts from the images onboard the SWIFTs. Most of breaking, rather, is in the offshore front on May 25th, and this is coincident with elevated near surface turbulent dissipation rates $\epsilon(z)$ that persist from $x = -25$ to -50 km while the SWIFT remains caught in the front. The maximum turbulent dissipation values are $\epsilon(z) \sim 3 \times 10^{-3}$ W/kg in the front on May 25th.

3.3. Scaling the wave breaking turbulence

As shown in previous studies (e.g., *Agrawal et al.* [1992]; *Gemmrich* [2010]; *Thomson et al.* [2013]), the high turbulent dissipation rates associated with wave breaking decay rapidly beneath the surface. In Figure 2, $\epsilon(z)$ reduces from 3×10^{-3} to 1×10^{-4} W/kg within a half meter below the surface. The vertical decay is important for evaluating the impact of wave-breaking turbulence on plume processes.

The canonical model for the vertical scaling of turbulence $\epsilon(z)$ generated during wave breaking is from *Terray et al.* [1996]. This model uses the wind stress as the TKE input term (assuming equilibrium, i.e., *Phillips* [1985]; *Thomson et al.* [2013]) and the significant wave height H_s as the vertical scale. This model was recently modified by *Feddersen* [2012a] to use observed wave energy flux gradients, dF/dx, as the TKE input term and by *Feddersen* [2012b] to use total water depth as the vertical scale (for surf zone applications). For the deep-water wave breaking observed at the Columbia Plume front, we apply the version based on observed wave energy gradients and significant wave heights,

$$\frac{\epsilon H_s}{dF/dx} = \alpha \left(\frac{z}{H_s}\right)^{-\lambda}, \tag{6}$$

in which α and λ are coefficients to be determined.

Figure 3 shows the results of the *Feddersen* [2012a] model with best-fit values rounded to $\alpha = 0.01$ and $\lambda = 1$. The departure from the more typical $\lambda = 2$ is expected in a region where downwelling is strong, and this result is consistent with other measurements during intense breaking (e.g., Zippel and Thomson, J. Geophys. Res., manuscript in revision). This scaling is used to extrapolate below the deepest values of the SWIFT estimates ($z = -0.6$ m) and assess the potential for breaking waves to elevate the turbulent mixing at the sub-surface interface of plume water and ocean water. Using the depth of maximum shear from Figure 2 as the plume depth, the extrapolated ϵ values at the interface are in the range of 10^{-6} to 10^{-5} W/Kg without breaking waves and 10^{-5} to 10^{-4} W/Kg with breaking waves. The values with breaking waves are in the range of the frontal values reported by *Kilcher and Nash* [2010].

4. Discussion

These observations clearly show that the plume front has a significant effect on short surface waves, if they are present and are energetic enough to reach steepness-limited breaking conditions. This mechanism significantly increases turbulence at the front, especially near the surface, where it may increase the vertical exchange of surface-bound material, organisms and even gases. However, the influence of this turbulence on mixing beneath the front is not known. Extrapolated turbulence dissipation rates suggest that wave-breaking turbulence may reach the depths where stratification is significant. The breaking generated turbulence at the plume front has a much deeper penetration ($\lambda = 1$ as best-fit to Eq. 6) than typically observed in the open ocean ($\lambda \approx 2$). It is likely that downward transport is enhanced at the plume front, where vertical velocities on the order of 0.2-0.4 m/s are often observed [*Orton and Jay*, 2005; *O'Donnell et al.*, 1998]. It also is possible that turbulent transport is stronger when the breaking is particularly regular and vigorous (as opposed to weak and intermittent whitecaps in the open ocean).

Although this study lacks direct observations of mixing or comprehensive characterization of the plume, a bulk estimate of mixing does provide additional context for these observations. Previous studies have used drifters to estimate bulk mixing levels in plumes using a Lagrangian control volume for salt, approximated by $h_p u \frac{ds}{dx}$, where h_p is the plume depth estimated as the level of maximum shear, u is the drifter velocity and $\frac{ds}{dx}$ is the change in salinity along the drifter track [*McCabe et al.*, 2008]. Applying this approach here results in estimates of $\epsilon \sim 10^{-4}$ W/Kg on May 24th and $\epsilon \sim 10^{-3}$ W/Kg on May

25th. This difference likely is related to the strong winds on May 25th, which in turn created the wind chop that broke at the plume front.

Two conditions are plausible for the wave breaking to lead to plume mixing. First, there could be strong stratification at the depths of high wave-driven TKE dissipation. Second, there could be significant downward diffusion (or transport) of wave-driven TKE to the depths of high stratification (as suggested by Figure 3). The first condition would be consistent with the leading edge of the spreading plume as a thin (~ 1 m) slab that is vigorously mixed by wave breaking, such that it is rapidly thickened as it spreads. Previous observations of the Columbia River plume do suggest that stratification can be strong very close to the surface (e.g., *Kilcher and Nash* [2010] Figure 4b), though an equally strong region of stratification exists well below the surface. The second condition would be less efficient, but more consistent with most observations of large river plumes. High-resolution measurements of the vertical salinity structure across the plume front, not collected during this study, would be necessary to evaluate these scenarios.

5. Conclusion

Observations of the Columbia River plume indicate that short waves break upon encountering the currents at the edge of the plume. Much of this wave energy is converted to turbulence during breaking, as confirmed by comparing the gradient of the wave energy flux with direct observations of near surface turbulent dissipation rates in a model for the vertical distribution of turbulent dissipation. The turbulence penetrates deeper than the canonical dependence for ocean ocean wave breaking, and the difference is attributed to strong downwelling at the front. Extrapolation of the turbulence to the depths where the plume entrains ocean water raises the possibility that surface generated turbulence can elevate the mixing of an expanding river plume.

Acknowledgments.

Data used in this article are available under the data tab at http://apl.uw.edu/swift.

Joe Talbert and Alex deKlerk built and maintained the SWIFTs. The R/V Oceanus, R/V Point Sur, and F/V Westward provided logistical support to deploy and recover the SWIFTs, with help from Chris Bassett, Walt Deppe, Ben Reeder, and Michael Schwendeman. Dan MacDonald and Rob Hetland provided ideas and comments on the data analysis and the manuscript. Jonathan Nash and an anonymous reviewer aided in the interoperation of results.

This work was supported by the Office of Naval Research, as part of the Data Assimilation and Remote Sensing for Littoral Applications (DARLA) project and in coordination with the Rivers and Inlets (RIVET) program.

References

Agrawal, Y., E. A. Terray, M. A. Donelan, P. A. Hwang, A. J. W. III, W. M. Drennan, K. Kahma, and S. A. Krtaigorodski (1992), Enhanced dissipation of kinetic energy beneath surface waves, *Nature*, *359*, 219–220, doi:10.1038/359219a0.

Banner, M. L., A. V. Babanin, and I. Young (2000), Breaking probability for dominant waves on the sea surface, *J. Phys. Oceanogr.*, *30*, 3145–3160.

Chawla, A., and J. T. Kirby (2002), Monochromatic and random wave breaking at blocking points, *Journal of Geophysical Research: Oceans*, *107*(C7), 4–1–4–19, doi: 10.1029/2001JC001042.

Craig, P. D., and M. L. Banner (1994), Modeling wave-enhanced turbulence in the ocean surface layer, *J. Phys. Oceanogr.*, *24*, 2546–2559.

Dong, Z., and J. Kirby (2012), Theoretical and numerical study of wave-current interaction in strongly-sheared flows, *Coastal Engineering Proceedings*, *1*(33).

Feddersen, F. (2012a), Observations of the surfzone turbulent dissipation rate, *J. Phys. Oceanogr.*, *42*, 386–399.

Feddersen, F. (2012b), Scaling surf zone turbulence, *Geophys. Res. Lett.*, *39*(18 (L18613)), doi:10.1029/2012GL052970.

Gemmrich, J. (2010), Strong turbulence in the wave crest region, *J. Phys. Oceanogr.*, *40*, 583–595.

Gerbi, G. P., R. J. Chant, and J. L. Wilkin (2013), Breaking surface wave effects on river plume dynamics during upwelling-favorable winds, *Journal of Physical Oceanography*, *43*(9), 1959–1980, doi:10.1175/JPO-D-12-0185.1.

Gonzalez, F. I., and C. L. Rosenfeld (1984), Slar and in situ observations of ocean swell modifcation by currents and bathymetry at the Columbia River entrance, *IEEE Trans. on Geoscience and Remote Sensing*, *GE-22*(6), 598–603.

Herbers, T. H. C., P. F. Jessen, T. T. Janssen, D. B. Colbert, and J. H. MacMahan (2012), Observing ocean surface waves with GPS tracked buoys, *J. Atmos. Ocean. Tech.*, *29*, doi:10.1175/JTECH-D-11-00128.1.

Kassem, S., and H. T. Ozkan-Haller (2012), Forecasting the wave-current interactions at the mouth of the columbia river, or, usa, in *Proceedings of the 33rd International Conference on Coastal Engineering*, Santander, Spain.

Kilcher, L., and J. Nash (2010), Structure and dynamics of the Columbia River tidal plume front, *J. Geophys. Res.*, *115*(C05S90), doi:10.1029/2009JC006,066.

MacDonald, D. G., L. Goodman, and R. D. Hetland (2007), Turbulent dissipation in a near-field river plume: A comparison of control volume and microstructure observations with a numerical model, *J. Geophys. Res.*, *112*, C07,026, doi:10.1029/2006JC004,075.

McCabe, R. M., P. MacCready, and B. M. Hickey (2008), Ebb Tide Dynamics and Spreading of a Large River Plume, *J. Phys. Oceanog.*, *113*(C08027).

Mei, C. (1989), *The Applied Dynamics of Ocean Surface Waves*, *Advanced Series on Ocean Engineering*, vol. 1, World Scientific.

Nash, J., and J. Moum (2005), River plumes as a source of large-amplitude internal waves in the coastal ocean, *Nature*, *437*, 400–403, doi:10.1038/nature03936.

O'Donnell, J., G. O. Marmorino, and C. L. Trump (1998), Convergence and Downwelling at a River Plume Front, *J. Geophys. Res.*, *28*, 1481–1495.

Orton, P. M., and D. A. Jay (2005), Observations at the tidal plume front of a high-volume river outflow, *Geophys. Res. Lett.*, *32*, doi:10.1029/2005GL022,372.

Phillips, O. M. (1985), Spectral and statistical properties of the equilibrium range in wind-generated gravity waves, *J. Fluid Mech.*, *156*, 495–531.

Rusch, C., S. Zippel, M. Schwendeman, and J. Thomson (2014), Detecting breaking waves in video data, in *Oceans 2014 proceedings*, IEEE/MTS.

Terray, E., M. Donelan, Y. Agrawal, W. Drennan, K. Kahma, A. Williams, P. Hwang, and S. Kitaigorodskii (1996), Estimates of kinetic energy dissipation under breaking waves, *J. Phys. Oceanogr.*, *26*, 792–807.

Thomson, J. (2012), Wave breaking dissipation observed with SWIFT drifters, *Journal of Atmospheric and Oceanic Technology*, *29*(12), 1866–1882, doi:10.1175/JTECH-D-12-00018.1.

Thomson, J., A. Jessup, and J. Gemmrich (2009), Energy dissipation and the spectral distribution of whitecaps, *Geophys. Res. Let.*, *36*.

Thomson, J., E. A. D'Asaro, M. Cronin, E. Rogers, R. Harcourt, and A. Schcerbina (2013), Waves and the equilibrium range at Ocean Weather Station P, *J. Geophys. Res.*, *118*, 1–12.

Wiles, P., T. P. Rippeth, J. Simpson, and P. Hendricks (2006), A novel technique for measuring the rate of turbulent dissipation in the marine environment, *Geophys. Res. Let.*, *33*, L21,608.

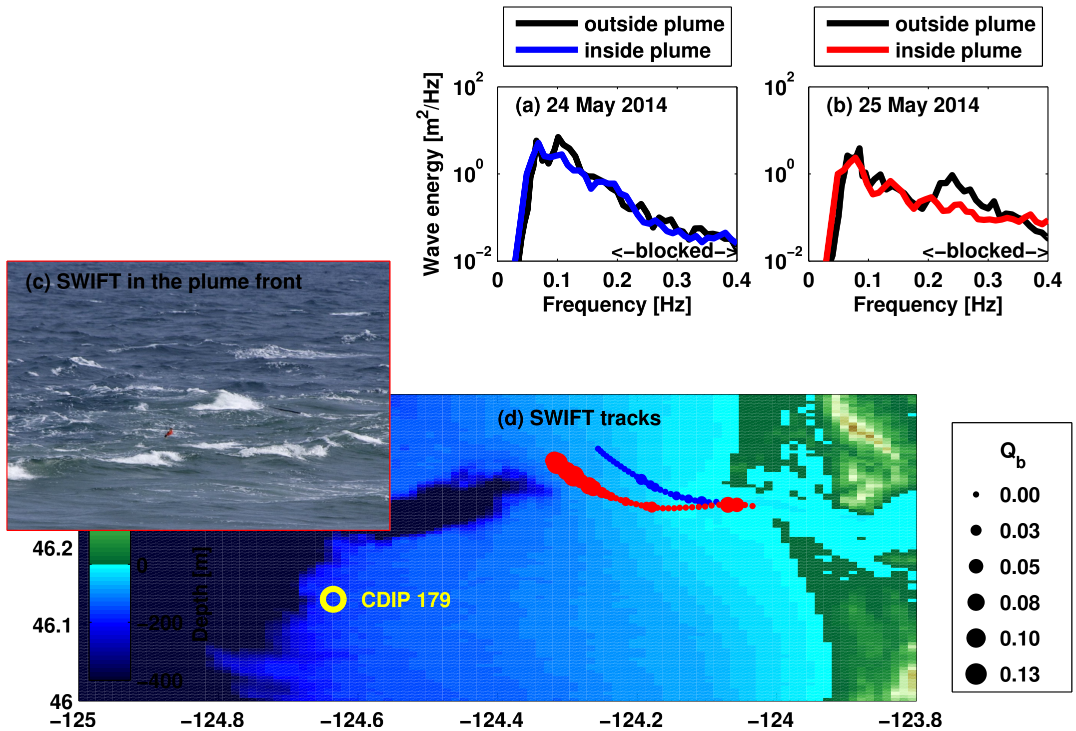

Figure 1. Wave energy spectra density versus frequency for 24 May 2014 (a) and 24 May 2014 (b). Red and blue lines are SWIFT measurements within the plume, and black lines are CDIP measurements outside of the plume. The frequencies at which waves are expected to break against the plume currents are shown with the annotation "blocked". (c) Photo of a SWIFT in the breakers at the offshore front. Photo taken by Chris Bassett on 28 May 2014, which was similar to 25 May 2014. (d) Tracks of SWIFT drifters as 5-minute average positions, colored by day (blue is May 24, red is May 25) and scaled by the fraction of breaking, Q_b.

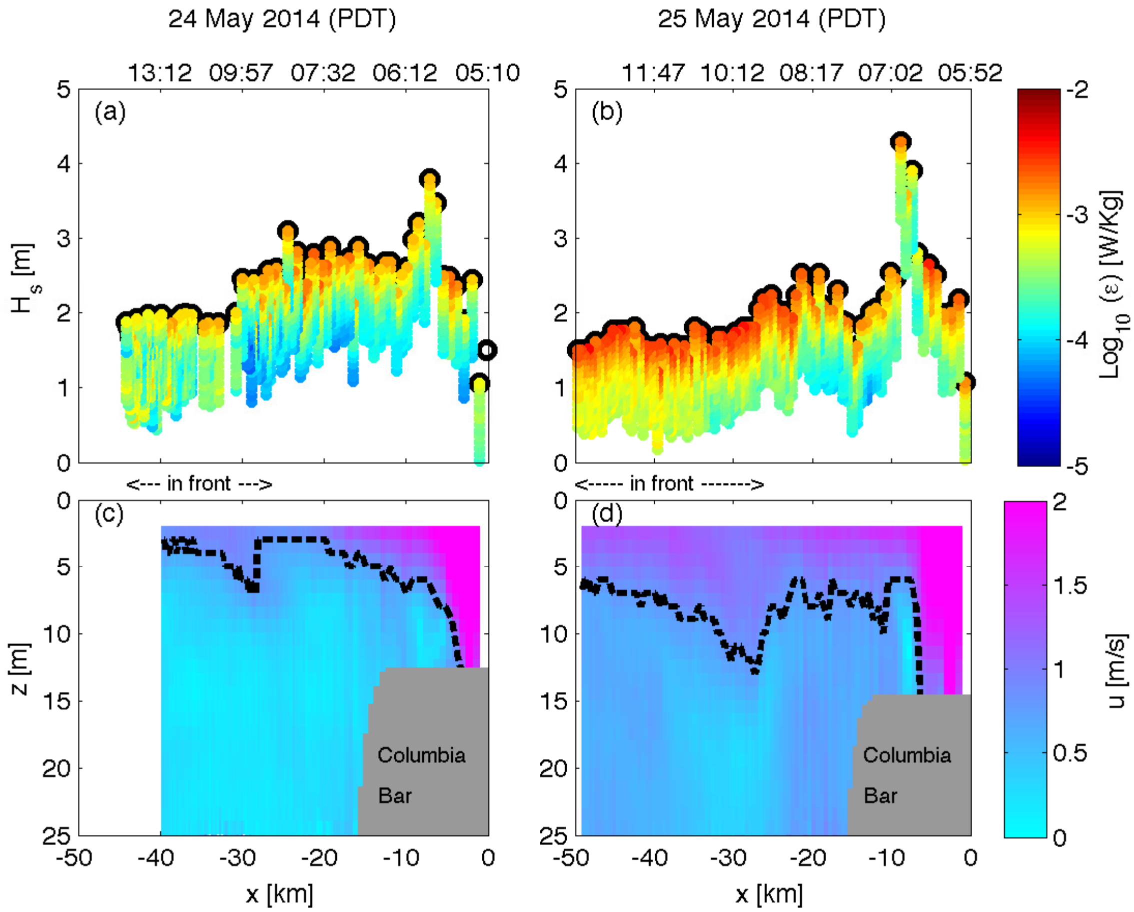

Figure 2. SWIFT results plotted versus local time and drift distance (along track distance offshore from river mouth) for a case without wave breaking (24 May 2014) and a case with wave breaking (25 May 2014). Significant wave height and vertical profiles of near surface turbulent dissipation rate (color scale) from the up-looking SWIFTs for (a) May 24 and (b) May 25th. Current profiles (color scale) and level of maximum shear from the down-looking SWIFTs for (c) May 24 and (d) May 25th. The SWIFTs are trapped in the plume front at approximately $x < -30$ km.

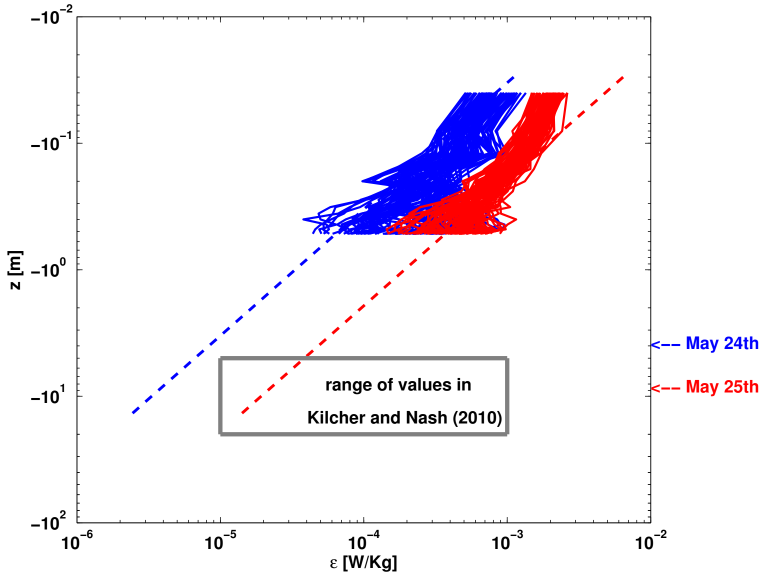

Figure 3. Observed (solid lines) and extrapolated (dashed lines) TKE dissipation rate profiles $\epsilon(z)$ from May 24 (blue) and May 25 (red). Also shown are the plume depths in the frontal region for both days, as well as the range of values reported in Kilcher & Nash [2010]. Near-surface TKE dissipation rates are enhanced by wave-breaking at the plume front on May 25, and the values extrapolated down to plume depths are within the range of sub-surface frontal values reported in *Kilcher and Nash* [2010]. Extrapolations use $\alpha = 0.01$ and $\lambda = 1$ in Eq. 6.